STUDY OF THE INFLUENCE OF AN ARTIFICIALLY FORMED PROTEIN CORONA ON THE SURFACE OF UPCONVERSION NANOPARTICLES ON THE UPTAKE EFFICIENCY BY MOUSE PERITONEAL MACROPHAGES

D.K. Bausheva, A.O. Belotelov, E.L. Guryev[*]

Institute of Biology and Biomedicine, Lobachevsky State University of Nizhny Novgorod, 23 Gagarin Ave., Nizhny Novgorod, 603950, Russia.

* Corresponding author: eguryev@ibbm.unn.ru

Abstract. The role of macrophages in nanomedicine is widely recognized, but systemically administered drug nanocarriers are rapidly absorbed and eliminated by the mononuclear phagocyte system, consisting of resident macrophages, primarily in the liver. As a result, most encapsulated drugs are eliminated from circulation, resulting in unwanted side effects. Peritoneal macrophages, on the contrary, by ingesting nanoparticles and migrating to tumor cells, can promote the antitumor effect. This article describes the preparation of complexes based on upconversion nanoparticles (UCNP) coated with nitrosonium tetrafluoroborate (NOBF4) with a protein corona (PC) from native and denatured bovine serum albumin (BSA and dBSA). The efficiency of UCNP-protein complexes uptake by mouse peritoneal macrophages has been demonstrated. The use of this approach is a promising area of oncology, since instead of inefficient systemic intravenous delivery, peritoneal delivery is used, which can become the key to solving the problem of peritoneal cavity cancers.

Keywords: upconversion nanoparticles, protein corona, macrophages.

List of Abbreviations

UCNP – upconversion nanoparticles
NOBF4 – nitrosonium tetrafluoroborate
PC – protein corona
BSA – bovine serum albumin
dBSA – denatured bovine serum albumin
PL – photoluminescence

Introduction

At the moment, theranostics is an actively developing area of biomedicine. Many nanomedicines have been developed for the purpose of diagnosing tumor foci and targeting tumor cells, as well as for controlling drug distribution and assessing the therapeutic effect (Kim *et al.*, 2009; Xie *et al.*, 2010; Grebenik *et al.*, 2016). However, general problems with the use of nanomedicines require solutions. Thus, it turned out that most of the nanomedicines introduced into the blood accumulate in the critical organs of the mononuclear phagocytic system – the liver and spleen – leading to difficult-to-remove toxicity (Bertrand *et al.*, 2014). There are also unwanted side effects caused by the basic effect of nanomedicines delivery – increased permeability and retention (EPR effect) (Maeda, 2010; Danhier, 2016).

After nanomedicines enter the body, proteins of the internal environment are actively adsorbed on their surface, which leads to the formation of a protein corona (PC) (Corbo *et al.*, 2016; Peng & Mu, 2016). The process of protein adsorption on the surface of nanomedicines is influenced by the affinity between proteins and nanomedicines, as well as between the proteins of the medium and proteins already adsorbed on nanomedicines (Monopoli *et al.*, 2012). PC significantly changes the initial physicochemical properties of nanomedicines and their "biological identity", affects the interaction with cells and the effects of nanomedicines in the body.

To date, data have been obtained on the possibility of using a preformed protein corona to stabilize and increase the circulation time of nanoparticles using albumin, transferrin, apolipoproteins and other proteins. Albumin is most often used for these purposes (Casals *et al.*, 2010). It is biocompatible, biodegradable, non-toxic, non-immunogenic and capable of long-term

circulation in the bloodstream (15-19 days) (Sleep *et al.*, 2013). The properties of albumin make it a potential stabilizer for nanoparticles, since it is adsorbed on their surface and forms a protein corona tightly bound to the surface of nanoparticles via electrostatic bonds (An & Zhang, 2013).

The two types of albumin most commonly used to create nanoparticle-based complexes are human serum albumin (HSA) and bovine serum albumin (BSA). HSA and BSA are homologous proteins. They share many characteristics, including molecular weight (65–70 kDa), high water solubility, and long half-life in the blood. Many cancer cells use albumin as a source of energy and nutrients (Stehle *et al.*, 1997) and typically exhibit increased albumin uptake via macropinocytosis (Commisso *et al.*, 2013).

When choosing a platform for creating theranostic complexes, special attention is paid to the use of upconversion nanoparticles (UCNPs). UCNPs are inorganic photoluminescent (PL) nanoparticles that have exceptional resistance to photo- and chemical degradation and excitation by wavelengths falling within the "transparency window" of biological tissue (Wang *et al.*, 2010, Aires *et al.*, 2015). These properties make it possible to create UCNP-based theranostic agents that have both diagnostic and therapeutic properties, which contributes to the search for new solutions in tumor therapy.

One of the solutions to the problem of insufficient efficiency of targeted delivery of nanomedicines in the case of tumors of the abdominal cavity and pelvic organs may be intraperitoneal administration. In this case, nanomedicines will practically not enter the systemic circulation and be absorbed by liver macrophages. Their absorption by macrophages lining the peritoneal cavity, on the contrary, is desirable. In this case, peritoneal macrophages, activated by inflammation caused by the tumor environment, can deliver nanomedicines to peritoneal tumor sites. Therefore, it is important to evaluate the ability of different nanocarriers to be taken up by peritoneal macrophages depending on their surface properties and particle sizes. In this work, we investigated the effects of an artificially formed protein corona of BSA and thermally denatured BSA (dBSA) on the surface of UCNPs on the efficiency of phagocytosis by peritoneal macrophages.

Materials and Methods

Obtaining and Characterization of UCNP

UCNP with core/shell structure $NaY_{0,794}Yb_{0,2}Tm_{0,006}F_4/NaYF_4$ were synthesized by the solvothermal decomposition as described earlier (Guryev *et al.*, 2020). The PL emission spectrum of UCNPs was studied using a spectrofluorimeter CM 2203 (SOLAR, Belarus). PL UCNPs were excited using a semiconductor laser generating radiation at a wavelength of 980 nm (Semiconductor Devices JSC, Russia).

Hydrophilic UCNPs were prepared by ligand exchange method (Dong *et al.*, 2011). Hydrophobic UCNPs in hexane (Kriochrome, Russia) were mixed with a solution of $NOBF_4$ in dimethylformamide (PanEco, Russia) in a ratio of 60 mg $NOBF_4$: 25 mg UCNP. The mixture was stirred overnight on a magnetic stirrer at room temperature. The mixture was centrifuged at 10,000 g for 7 min, UCNP was resuspended in dimethylformamide, and a hexane/toluene mixture (1:1) (Khimreaktiv, Russia) was added. The UCNPs were then washed with ethanol twice and resuspended in deionized water. The hydrodynamic diameter of the particles was measured by dynamic light scattering using a Zetasizer Nano ZS system (Malvern, UK).

Preparation of UCNP-protein complexes

UCNPs with stable PC from BSA and dBSA on the surface of nanoparticles were prepared by lyophilization as described earlier (Shanwar *et al.*, 2021). The BSA solution was incubated for 30 min at 70 °C to obtain dBSA. The UCNP-$NOBF_4$ suspension (0.5 mg/mL) was added dropwise to the BSA and dBSA solutions (100 μM) with stirring. The mixture was incubated at room temperature for 4 h. UCNP-$NOBF_4$-BSA and UCNP-$NOBF_4$-dBSA samples were lyophilized using a FreeZone 6L device (Labconco, USA). Samples were placed in

glass vials and frozen at -80 °C, then kept in a lyophilization chamber at -50 °C under high vacuum for 24 h until the water was completely removed. Lyophilized samples were stored at 4 °C.

Study of the circulation time of UCNP-$NOBF_4$ and UCNP-$NOBF_4$-BSA in the blood of laboratory animals

A series of dilutions of UCNP-$NOBF_4$ and UCNP-$NOBF_4$-BSA were prepared with concentrations of 5, 20, 40, 60, 80, 100 μg/ml in heparinized blood. The PL signal intensity was measured using a UCNP imaging device DVS-02 as described previously (Guryev *et al.*, 2019). Based on these data, calibration graphs of the dependence of the PL signal intensity on the UCNP concentration were obtained.

The studied particles and complexes in an amount of 200 μg in 200 μl of PBS were injected to Balb/c mice into the left lateral tail vein (the first two-thirds of the length of the vein from the tip of the tail). Blood samples were taken from the retrobital sinus at 0.5, 1.5, 2, 3, 4, 5, 10, 15 and 30 min after the administration of particles and complexes. Samples were diluted with heparin in the ratio 25 μl (blood) : 15 μl (heparin). The intensity of the PL signal of UCNP in the samples was measured using a DVS-02 device, the concentration of particles and complexes was calculated using calibration graphs.

Study of the complexes uptake efficiency by peritoneal macrophages

Macrophages were isolated from the peritoneal transudate of Balb/C mice, the complexes uptake was studied *in vitro*. Cells were seeded into the wells of a 96-well confocal plate and incubated for 12 h. After incubation of the peritoneal cell suspension in the wells of the plate, the culture medium was removed, which removed the majority of non-macrophage peritoneal cells. Wells with macrophages attached to the bottom were washed with PBS, 1 ml of a suspension of UCNP-$NOBF_4$-BSA or UCNP-$NOBF_4$-dBSA (0.2 mg/ml in PBS) was added to the wells, and incubated for 2 h. The suspension was removed and the wells were washed with PBS. Cells were fixed with 4% formaldehyde for 30 min and washed with PBS and deionized water. The preparations were examined by confocal laser fluorescence microscopy. Quantitative data were processed using the program GraphPad Prism 6 (GraphPad Software, США)

Results

Obtaining and Characterization of UCNP

Using the solvatothermal decomposition method, UCNPs were obtained based on a $NaYF_4$ matrix doped with ytterbium and thulium lanthanide ions. Inert $NaYF_4$ shell reduces surface quenching effects and increases UCNP PL intensity (Grebenik *et al.*, 2016). Such UCNPs exhibit anti-Stokes PL with pronounced emission maxima in the visible (around 474 nm) and near-infrared (IR) spectral regions (around 801 nm) when excited by light with a wavelength of 980 nm (Fig. 1). The main maximum of PL emission is in the IR region and falls within the transparency window of the biological tissue. This makes UCNPs doped with thulium ions effective agents for bioimaging at the level of tissues, organs and the whole body of small laboratory animals.

Nitrosonium tetrafluoroborate ($NOBF_4$) coated UCNPs were prepared using the ligand exchange method (Fig. 2). Such a shell makes it possible to obtain a monodisperse suspension of colloidally stable biocompatible particles (Dong *et al.*, 2011). The hydrodynamic diameter of the UCNP-$NOBF_4$ particles was 54.80 ± ± 20.34 nm (Fig. 3), and the polydispersity index (PDI) was 0.229, indicating the homogeneity of the sample.

Preparation of UCNP-protein complexes

UCNPs with stable PC from BSA and dBSA on the surface of nanoparticles were obtained by lyophilization using previously developed technique (Shanwar *et al.*, 2021). The use of native BSA in optimal concentration allows the formation of a stable protein layer that completely covers the surface of the particles, which makes the suspension colloidally stable (Fig. 2). An excess or deficiency of protein molecules leads to increased aggregation.

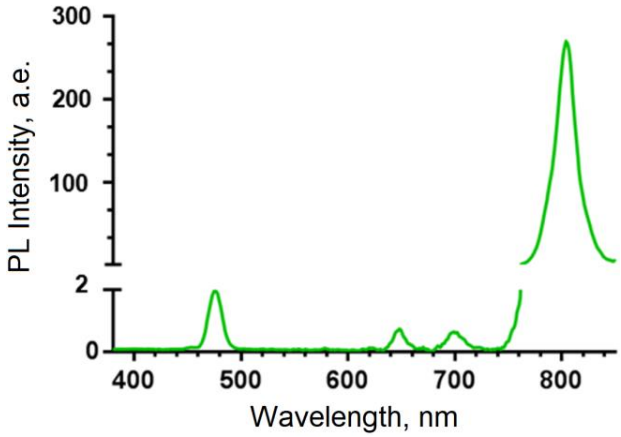

Fig. 1. Emission spectrum of PL UCNPs with the composition $NaYF_4$:Yb:Tm/$NaYF_4$ when excited by light with a wavelength of 980 nm

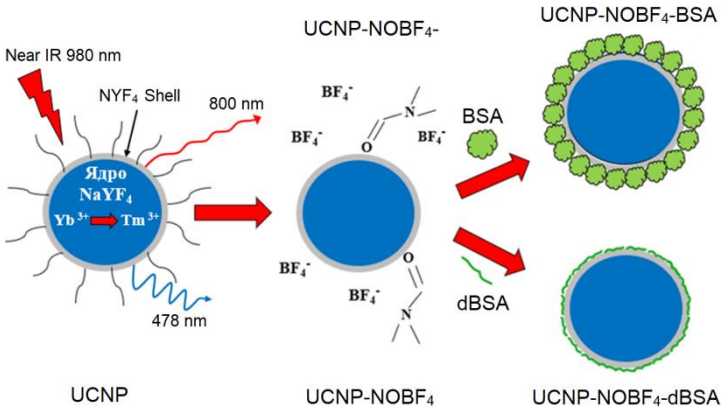

Fig. 2. Scheme for converting hydrophobic UCNP-Oleate into biocompatible UCNP-$NOBF_4$ by exchanging ligands and obtaining UCNPs with an artificially formed protein corona of BSA and dBSA

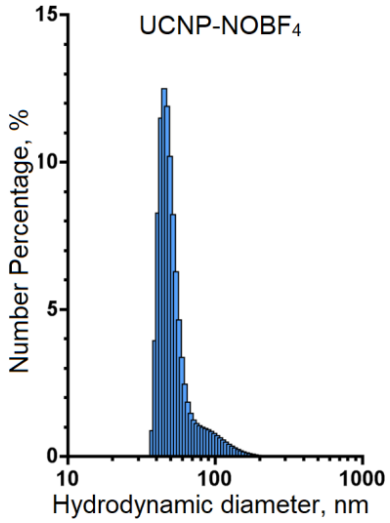

Fig. 3. Hydrodynamic diameter of UCNP-$NOBF_4$ particles

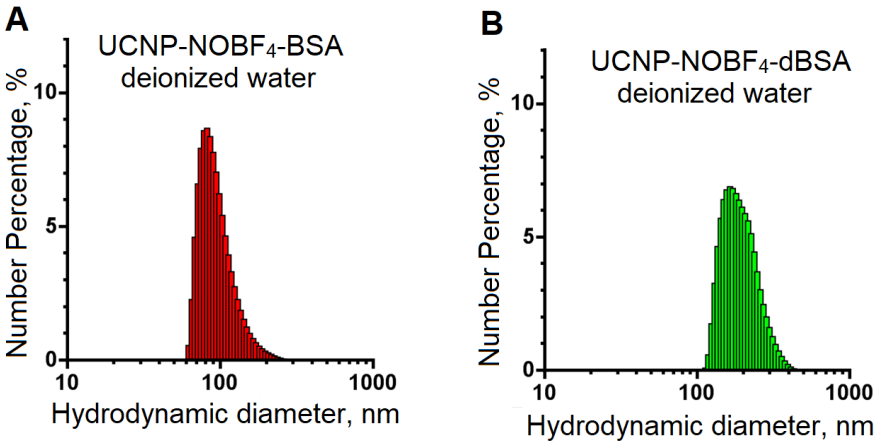

Fig. 4. Hydrodynamic diameter of UCNP-$NOBF_4$-BSA (A) and UCNP-$NOBF_4$-dBSA (B) in deionized water

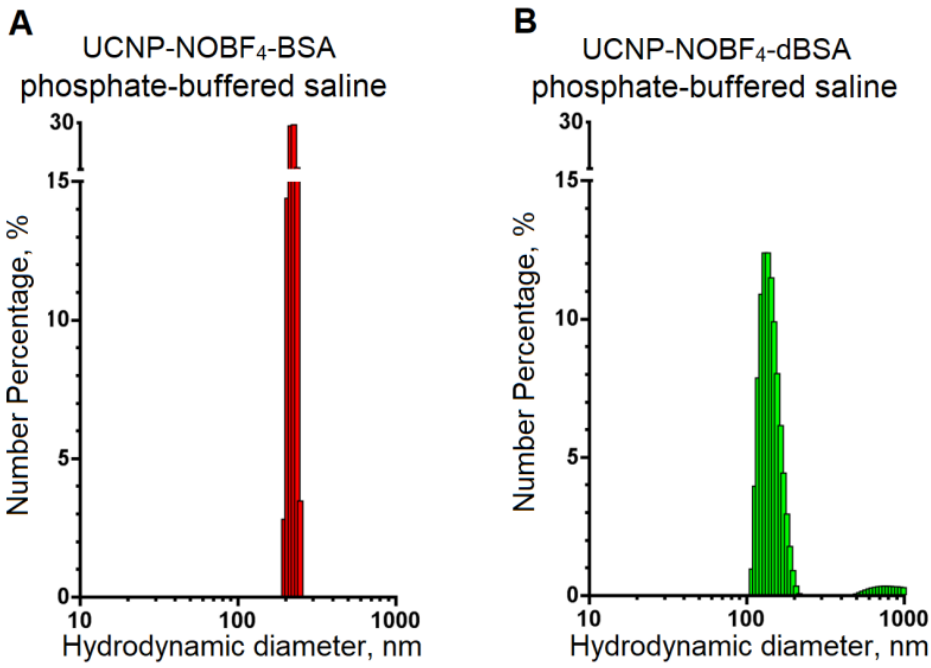

Fig. 5. Hydrodynamic diameter of UCNP-$NOBF_4$-BSA and UCNP-$NOBF_4$-dBSA in phosphate-buffered saline

The use of denatured BSA allows for thinner and denser PC due to the unfolding of the BSA peptide chain. Also, epitopes of the BSA molecule, hidden inside the globule in the native state, are exposed.

The hydrodynamic diameter of UCNP-$NOBF_4$-BSA particles resuspended in deionized water was 96.33 ± 27.25 nm (Fig. 4A). The PDI was 0.216, indicating that the sample was homogeneous. The hydrodynamic diameter of UCNP-$NOBF_4$-dBSA particles in deionized water was 195.4 ± 52.32 nm (Fig. 4B), PDI was 0.116, which also indicates the homogeneity of the sample.

The hydrodynamic diameter of UCNP-$NOBF_4$-BSA particles resuspended in phosphate-buffered saline was 221.7 ± 11.59 nm (Fig. 5A), PDI 0.616. The hydrodynamic diameter of UCNP-$NOBF_4$-dBSA particles in phosphate-buffered saline was 141.7 ± 19.46 nm,

and there was also a small peak at 851.9 ± 235.4 (Fig. 5B), and the PDI was 0.613, indicating sample heterogeneity and partial aggregation of particles.

Study of the circulation time of UCNP-$NOBF_4$ and UCNP-$NOBF_4$-BSA in the blood of laboratory animals

To assess the effect of the PC on the behavior of particles in the body upon systemic administration, a study of UCNP of removal rate from the mice bloodstream was performed. A suspension of UCNP-$NOBF_4$ and UCNP-$NOBF_4$-BSA was injected into the left lateral tail vein, and blood samples were collected from the retrobital sinus. Measuring the intensity of the PL signal of blood samples made it possible to identify a single-exponential dependence of the content of particles and complexes in the blood on time (Fig. 6). During the first minutes after administration, a rapid decrease in the concentration of particles and complexes in the blood was observed. The half-life of UCNP-$NOBF_4$ particles calculated by interpolation was 2.621 min, UCNP-$NOBF_4$-BSA complexes – 0.799 min. This value refers to the time required for the concentration of the test compound to decrease by half at any time point after administration. At the last time point (30 min), the concentration of particles and complexes in the blood approaches zero.

Study of the complexes uptake efficiency by peritoneal macrophages

The macrophage fraction from the peritoneal transudate of Balb/C mice was isolated by sequential washing of peritoneal cells and morphological assessment. As a result of incubation of UCNP-protein complexes with peritoneal macrophages and microscopic examination, a greater accumulation of UCNP-$NOBF_4$-BSA complexes in peritoneal macrophages was shown compared to UCNP-$NOBF_4$-dBSA. The micrographs show a significant PL signal of UCNP in areas of the field of view occupied by cells incubated with UCNP-$NOBF_4$-BSA complexes (Fig. 7). In the case of UCNP-$NOBF_4$-dBSA complexes, the PL signal in the cell area is weakly expressed.

To confirm the obtained microscopy results, a quantitative assessment of the PL signal level in the areas of the visual field occupied by cells was carried out (Fig. 8). Data analysis using the Kruskal-Wallis test showed a statistically significant difference in the intensity of the PL signal of UCNP in the first group (UCNP-NOBF4-BSA) from the other two studied groups of images ($p < 0.05$).

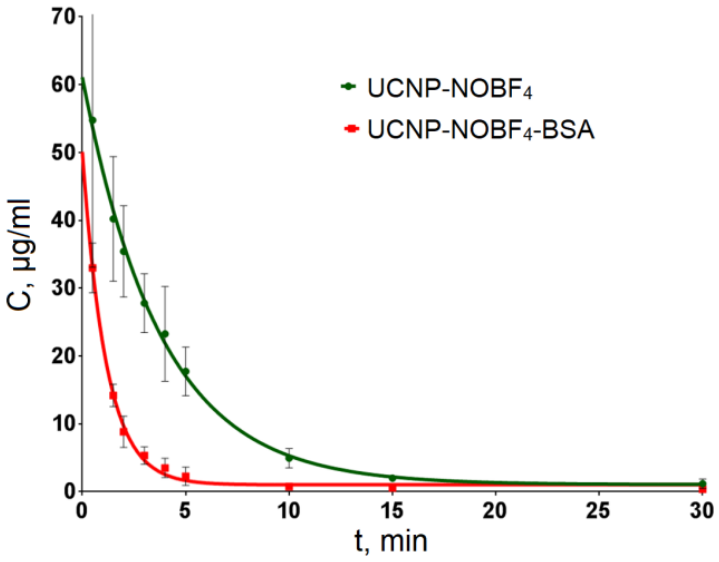

Fig. 6. Concentration of UCNP-$NOBF_4$ particles and UCNP-$NOBF_4$-BSA complexes in mouse blood when administered intravenously at a dose of 10 mg/kg

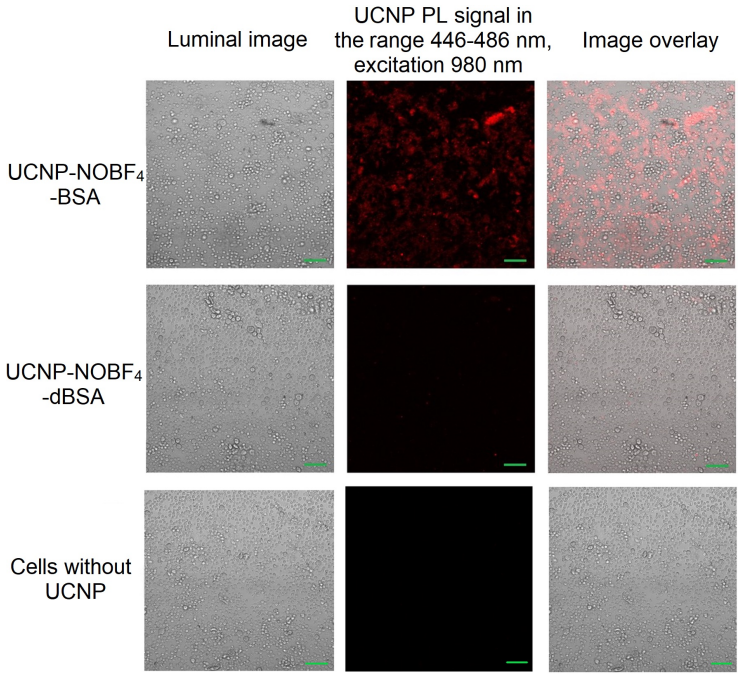

Fig. 7. Micrographs obtained by confocal fluorescence microscopy: peritoneal macrophages incubated for 2 h with UCNP-$NOBF_4$-BSA and UCNP-$NOBF_4$-dBSA complexes and peritoneal macrophages without UCNP. Scale bar: 50 μm. The PL signal of UCNP is shown in red

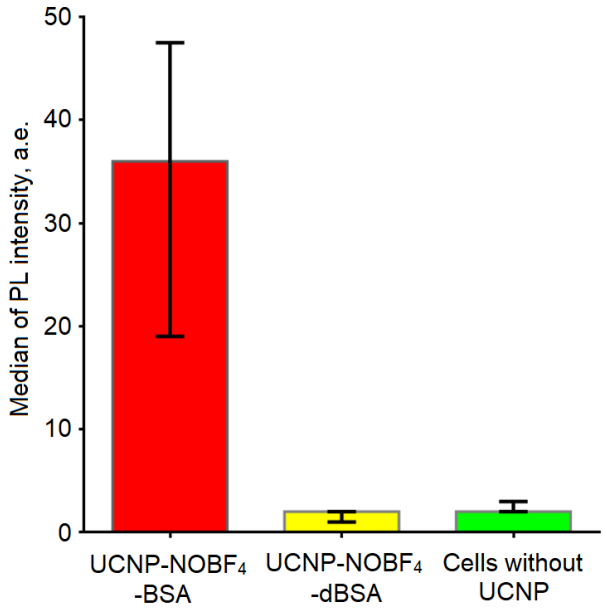

Fig. 8. Median values of the intensity of the PL signal of UCNP-$NOBF_4$-BSA and UCNP-$NOBF_4$-dBSA complexes and peritoneal macrophages without particles. Error bars are represented by the interquartile range. n = 25

Discussion

While local drug concentrations in tumor tissue can be increased through the use of passive delivery, active delivery to a specific cell type through targeting agents can in some cases further improve the effectiveness of the targeted drug. Typically, such strategies do not increase the total concentration in the target tissue, but

rather alter the distribution within the tissue, increasing the selectivity of the drug and minimizing side effects. It is expected that the intraperitoneal administration method will overcome the lack of efficiency of targeted delivery of nanomedicines. In this case, nanomedicines will not be quickly removed from the bloodstream by cells of the mononuclear phagocytic system and accumulate in the liver and spleen.

In the present work, complexes of biocompatible UCNPs with BSA were prepared. The obtained results of measuring the hydrodynamic diameter of the complexes allow us to count on their effective use for delivery to tumor sites, since they remain fairly small in size and do not demonstrate significant aggregation. Such particles, when administered intraperitoneally, can be absorbed by macrophages and, with their help, delivered to tumor sites. It is obvious that the behavior of complexes in water or a buffer solution differs from that in the internal environment of the body. On the other hand, an increase in particle size due to possible aggregation enhances their uptake by macrophages rather than weakens it.

The coating of the particles with BSA was carried out in order to reduce the adsorption of proteins from the internal environment of the body. Several studies have shown that this coating increases the circulation time of particles in the bloodstream. In contrast, our data showed faster clearance of BSA-coated particles compared to the original UCNP-$NOBF_4$. A possible reason for the observed effect may be partial denaturation of BSA molecules during lyophilization, which leads to increased uptake of particles by liver macrophages and reduces their circulation time in the bloodstream.

In the case of intraperitoneal administration of the resulting complexes, their increased uptake by macrophages, on the contrary, is desirable. The results of the study showed greater accumulation of UCNP-$NOBF_4$-BSA in peritoneal macrophages compared to UCNP-$NOBF_4$-dBSA. This may be explained by the larger size of UCNP-$NOBF_4$-BSA complexes as well as the recognition of native BSA epitopes by peritoneal macrophages as signals to engulf objects bearing these epitopes. We hypothesize that these macrophages play a key role in the delivery of nanomedicines to tumor nodes, and our findings will contribute to the development of mechanisms for enhancing the therapeutic effect of antitumor therapy using macrophages.

Acknowledgments

This research was supported by the Ministry of Science and Higher Education of the Russian Federation, project No. FSWR-2023-0032.

References

AIRES A., OCAMPO S.M., CABRERA D., CUEVA L. DE LA., SALAS G., TERAN F.J. & CORTAJARENA A.L. (2015): BSA-coated magnetic nanoparticles for improved therapeutic properties. *Journal of Materials Chemistry B* **3**(30), 6239–6247.

AN F.F. & ZHANG X.H. (2017): Strategies for Preparing Albumin-based Nanoparticles for Multifunctional Bioimaging and Drug Delivery. *Theranostics* **7**(15), 3667–3689.

BERTRAND N., WU J., XU X., KAMALY N. & FAROKHZAD O.C. (2014): Cancer nanotechnology: The impact of passive and active targeting in the era of modern cancer biology. *Advanced Drug Delivery Reviews* **66**, 2–25.

CASALS E., PFALLER T., DUSCHL A., OOSTINGH G.J. & PUNTES V. (2010): Time evolution of the nanoparticle protein corona. *ACS Nano* **4**(7), 3623–3632.

COMMISSO C., DAVIDSON S.M., SOYDANER-AZELOGLU R.G., PARKER S.J., KAMPHORST J.J., HACKETT S. ET AL. (2013): Macropinocytosis of protein is an amino acid supply route in Ras-transformed cells. *Nature* **497**, 633–637.

CORBO C., MOLINARO R. & PARODI A. (2016): The impact of nanoparticle protein corona on cytotoxicity, immunotoxicity and target drug delivery. *Nanomedicine* **11**(1), 81–100.

DANHIER F. (2016): To exploit the tumor microenvironment: Since the EPR effect fails in the clinic, what is the future of nanomedicine? *J. Controll. Release* **244**, 108–121.

DONG A., YE X., CHEN J., KANG Y., GORDON T., KIKKAWA J.M. ET AL. (2011): Generalized Ligand-Exchange Strategy Enabling Sequential Surface Functionalization of Colloidal Nanocrystals. *J. Am. Chem. Soc.* **133**(4), 998–1006.

GREBENIK E.A., KOSTYUK A.B. & DEYEV S.M. (2016): Upconversion nanoparticles and their hybrid assemblies for biomedical applications. *Russ. Chem. Rev*. **85**(12), 1277–1296.

GURYEV E.L., SHILYAGINA N.Y., KOSTYUK A.B., SENCHA L.M., BALALAEVA I.V., VODENEEV V.A. ET AL. (2019): Preclinical Study of Biofunctional Polymer-Coated Upconversion Nanoparticles. *Toxicological Sciences* **170**(1), 123–132.

GURYEV E.L., SMYSHLYAEVA A.S., SHILYAGINA N.Y., SOKOLOVA E.A., SHANWAR S., KOSTYUK A.B. ET AL. (2020): UCNP-based Photoluminescent Nanomedicines for Targeted Imaging and Theranostics of Cancer. *Molecules* **25**(18), 4302.

KIM J., PIAO Y. & HYEON T. (2009): Multifunctional nanostructured materials for multimodal imaging, and simultaneous imaging and therapy. *Chem. Soc. Rev* **38**(2), 372–390.

MAEDA H. (2010): Tumor-selective delivery of macromolecular drugs via the EPR effect: background and future prospects. *Bioconj. Chem*. **21**(5), 797–802.

MONOPOLI M.P., ÅBERG C., SALVATI A. & DAWSON K.A. (2012): Biomolecular Coronas Provide the Biological Identity of Nanosized Materials. *Nat. Nanotechnol.* **7**, 779–786.

PENG Q. & MU H. (2016): The potential of protein-nanomaterial interaction for advanced drug delivery. *J. Controll. Release* **225**, 121–132.

SHANWAR S., LIANG L., NECHAEV A.V., BAUSHEVA D.K., BALALAEVA I.V., VODENEEV V.A. ET AL. (2021): Controlled Formation of a Protein Corona Composed of Denatured BSA on Upconversion Nanoparticles Improves Their Colloidal Stability. *Materials* **14**(7), 1657.

SLEEP D., CAMERON J. & EVANS L.R. (2013): Albumin as a versatile platform for drug half-life extension. *Biochim. Biophys. Acta* **1830**(12), 5526–5534.

STEHLE G., SINN H., WUNDER A., SCHRENK H.H., STEWART J.C, HARTUNG G. ET AL. (1997): Plasma protein (albumin) catabolism by the tumor itselfeimplications for tumor metabolism and the genesis of cachexia. *Crit. Rev. Oncol. Hematol* **26**, 77–100.

WANG F., WANG J. & LIU X. (2010): Direct Evidence of a Surface Quenching Effect on Size-Dependent Luminescence of Upconversion Nanoparticles. *Angewandte Chemie International Edition* **49**(41), 7456–7460.

XIE J., LEE S. & CHEN X. (2010): Nanoparticle-based theranostic agents. *Advanced Drug Delivery Reviews* **62**, 1064–1079.